

Quantifying relationship between relative position error of localization algorithms and object identification

Noboru Kiyama · Akira Uchiyama ·
Hirozumi Yamaguchi · Teruo Higashino

Published online: 30 October 2012
© Springer Science+Business Media New York 2012

Abstract Positioning of things, devices and people is the fundamental technology in ubiquitous computing. However, few literature has discussed the impact of positioning errors due to localization algorithm properties such as ranging noise and deployment of anchors on people's identification of objects. Since several factors such as relative distance, relative angles and grouping of objects are intricately related with each other in such identification, it is not an easy task to investigate its characteristics. In this paper, we propose criteria to assess the “accuracy” of the estimated positions in identifying the objects. The criteria are helpful to design, develop and evaluate localization algorithms that are used to tell people the location of objects. Augmented reality is a typical example that needs such localization algorithms. To model the criteria without ambiguity, we prove that the Delaunay triangulation well-captures natural human behavior of finding similarity between estimated and true positions. We have examined different localization algorithms to observe how the proposed model quantifies the properties of those algorithms. Subjective testing has also been conducted using questionnaires to justify our quantification sufficiently renders human intuition.

Keywords Relative positioning · Localization · Object identification · Delaunay triangulation

1 Introduction

Positioning systems have been investigated so far for location-aware services such as outdoor/indoor navigation and personal object identification in rooms. GPS is the most popular global system for outdoor positioning of single nodes. For the situation where GPS is not available, localization algorithms using a variety of devices have been developed. In wireless sensor networks, cooperative self-localization is mandatory since in most cases we cannot attach GPS to small-sized wireless sensor nodes due to limitation of cost and battery lifetime. Some other services such as support of social interaction [1] and indoor navigation for emergency service [2] need positioning of mobile nodes.

In those applications, the accuracy of position information is highly significant. In particular, we focus on such applications that need identification of real objects from position information. Let us suppose an AR (augmented reality) system in a huge storehouse that shows article IDs over camera views by balloons using the estimated positions of those articles (Fig. 1). The errors from the positioning system may directly appear as the deviation of ID balloons from the true positions in the camera views. Although case 1 (Fig. 1(a)) and case 2 (Fig. 1(b)) have similar amounts of deviations from the true positions, most people may not be able to find the correct matching in case 2 where switching of B and C is likely to occur (or even A and B). This is obviously because the relative location of B and C (and also A and B) is quite different from the truth.

As seen, such errors that cause mismatching between estimated positions and truth should be represented not

N. Kiyama (✉) · A. Uchiyama · H. Yamaguchi · T. Higashino
Graduate School of Information Science and Technology,
Osaka University, 1-5 Yamadaoka, Suita, Osaka 5650871, Japan
e-mail: n-kiyama@ist.osaka-u.ac.jp

A. Uchiyama
e-mail: utiyama@ist.osaka-u.ac.jp

H. Yamaguchi
e-mail: h-yamagu@ist.osaka-u.ac.jp

T. Higashino
e-mail: higashino@ist.osaka-u.ac.jp

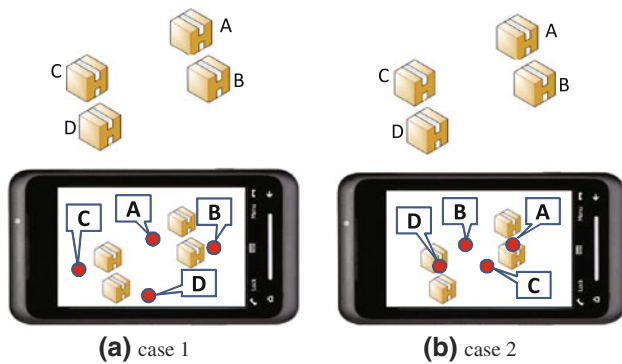


Fig. 1 Example of object identification in augmented reality: AR system shows article IDs over camera views by balloons using estimated positions of those articles. Most people may not be able to find the correct ID matching in **b** although **a** and **b** have similar errors from the positioning system

only by the deviation from the true positions but also by the deviation from the true *position relationship*. Although the term “relative position” partially captures the concept of position relationship, it does not take the impact on people’s object identification into consideration (namely, it is defined independently of application context). Therefore, our approach is differentiated from existing ones that have dealt with relative position accuracy [3, 4]. In brand-new mobile and pervasive applications that associate estimated location information obtained by positioning systems with the physical things, such an impact should be considered and thus some reasonable criteria are desired for the purpose.

In this paper, we focus on how to characterize the outputs by a localization algorithm and try to quantify the impact of positioning errors on people’s identification of objects independently of specific localization algorithms. Given a set of estimated positions of target objects and the anonymous set of their true positions, we propose criteria to access the “accuracy” of the estimated positions in identifying the objects at true positions. The proposed accuracy criteria can be used in design, development and evaluation of localization algorithms that are used to tell people the location of objects (augmented reality is a typical example). To define the criteria without ambiguity, we prove that (1) neighbor proximity and uniqueness are significant factors to identify objects and the Delaunay triangulation captures these properties, and (2) grouping of nearby neighbors should also be considered and properly-designed clustering captures the property. Then *position relationship dissimilarity* is defined by the degree of discrepancy (DoD) of Delaunay triangulations on estimated and true positions considering clusters.

In order to validate our approach, we have analyzed properties of three localization algorithms using the proposed criteria. The results have shown that the criteria could capture the qualitative properties of each algorithm.

Subjective testing has also been conducted using 120 questionnaires. Analyzing the obtained 6,480 answers from 54 examinees, we have confirmed that our quantification could sufficiently render human perception.

2 Related work

2.1 Relative position accuracy

There have been several researches that deal with relative position accuracy [3–5] in different research domains. For example, Ref. [5] in the computer vision research considers the correctness of relationship between two objects by shapes or directions in 2D or 3D space. However, these approaches do not consider the correctness of position estimation in terms of object identification.

Relative positioning accuracy analysis has been achieved in wireless sensor network localization by several papers like Refs. [3, 4]. Most of these papers dealing with relative positioning accuracy have focused on the *errors from the measurement*. Since the anchors are not concerned in relative positioning, errors are usually defined as deviation from the measurement such as distance, angles and RSS. Therefore, these approaches are different from ours since they do not take the impact on people’s object identification into account. In other words, they are defined independently of application context.

2.2 Localization algorithm classification

In Sect. 6, we have analyzed some existing localization algorithms by our proposed criteria. Before that section, we briefly address the classification of localization algorithms here. We note that this section is not intended to survey recent work on localization, but to introduce different types of localization algorithms.

Range-based localization techniques rely on distance estimation by received signal strength (RSS) to distance mapping, time of arrival (TOA) by ultrasound or audible sound, time difference of arrival (TDOA) in ultra wide band or simultaneous use of RF and ultrasound [6] and so on. Directional antennas are often used to estimate angle of arrival (AOA). Based on the ranging technique, this category can further be categorized into two different types of localization algorithms. Single node localization uses tri- or multi-lateration where distance or angle information from at least three reference points is used to determine the location (GPS falls into this category). Wi-Fi and/or cellular fingerprinting such as [7] also fall into this category. On the other hand, MDS-MAP [8] is a known algorithm for localizing multiple nodes simultaneously. It uses shortest path information or other ranging techniques to estimate

the distance, and uses “multidimensional scaling” to determine their positions.

Range-free techniques are cost effective alternatives since they only require communication function. Amorphous [9] is a well-known range-free algorithm that utilizes hop counts from landmarks, where each node estimates its coordinates by finding coordinates that minimize the total squared error between the calculated and estimated distances. TRADE [10] is a constraint-based algorithm to localize mobile nodes. It constrains the location of nodes from temporal–spatial information about wireless connectivity and movement, and estimates likely points from the region that satisfies the constraints.

2.3 Delaunay triangulation for similarity quantification

Pattern matching problems in image recognition deal with quantifying relationship between two objects. The basic algorithm usually consists of two processes; feature extraction and identification. The former process extracts significant points (e.g. a nose or eyes in facial recognition) from input data. The latter process quantifies these significant points by classifying or categorizing them. There are two types of identification in pattern matching problems. One is statistical pattern recognition which compares input data with enormous accumulated data. Another is structural pattern recognition which analyzes deployment of significant points obtained from input data. Therefore prior knowledge is not required. For example, in Ref. [11], eigenvectors are used for identification in facial recognition. In Ref. [12], singular points are used for identification in image matching. Ref. [13] obtains relationships between significant points using the Delaunay triangulations for identification in fingerprint matching. Ref. [14] proposed an algorithm to group points using reduced Delaunay graphs (RDGs). It is based on the Gestalt law of proximity in Gestalt psychology [15] that suggests the law of proximity as an important factor of grouping objects in human perception.

These approaches use the Delaunay triangulation to represent the feature amount of given images. Our approach is completely different in the sense that we aim at quantifying the relationship between localization errors and object identification, and use the Delaunay triangulation and clustering for such quantification.

2.4 Our contributions

To the best of our knowledge, this is the first approach that quantifies localization errors in the context of object identification. As briefly discussed in Sect. 1, the existing approaches that have dealt with relative position accuracy [3, 4] are different from ours in the sense that they consider

relative position errors, which are defined by distance among objects and relative angles. We can intuitively understand that the “relative position errors” may represent some features of algorithm performance in object identification, though discussion has not been given and corresponding criteria have not been quantitatively defined. Meanwhile, our approach considers several features in object identification, such as proximity–uniqueness property, clustering and viewpoints. Justification has been done by experiments and subjective test using questionnaires and a tool developed for this purpose. As stated in the previous section, the notion of Delaunay triangulation similarity is found in image recognition, but they use the Delaunay triangulations only to characterize point patterns. In other words, they use only the planer-graph property to characterize a point distribution on a 2D plane.

We believe that new mobile and pervasive applications like navigation of articles and people are beneficial from our approach to assess adequacy of positioning systems they use.

3 Basic approach

3.1 Concept

Position relationship dissimilarity between true and estimated positions is quantified by the Delaunay triangles in our approach. To imagine what should be considered in node identification, we introduce a simple example. Figure 2(a) shows real placement of nodes and Fig. 2(b), (c) show two different estimations. We assume these figures are drawn in bird’s-eye view. Compared with the true positions, the relative positions of nodes F and G in Fig. 2(c) are “opposite” from the viewpoint of node C , while those in Fig. 2(b) are consistent. In terms of relationship between C and the pair (F, G) , we may think Fig. 2(b) is “better” than Fig. 2(c).

We have also prepared 4 sets of node positions with errors as shown in Fig. 3 where the true positions are shown in Fig. 3(c). Each set is generated by adding 3 m error to the true position of each node in a 20 m \times 20 m square area. Therefore, the average position errors of those sets are the same. We note that solid lines indicate alphabetically consecutive node pairs ($H-A$ is also drawn) and arrows show the position errors. We can say that Fig. 3(a), (b) have certain similarity to the true positions rather than Fig. 3(d), (e) although their average errors are the same. Suppose identification of anonymous nodes at true positions by a given set of estimated positions like Fig. 3(a) as exemplified in Sect. 1. Obviously neither of Fig. 3(d), (e) is helpful for such a purpose because the position relationship among neighbors is hardly preserved. For example, in the

Fig. 2 Relative positions of *F* and *G* from bird’s-eye view: **a** real position, **b** “consistent” estimation, **c** “inconsistent” estimation

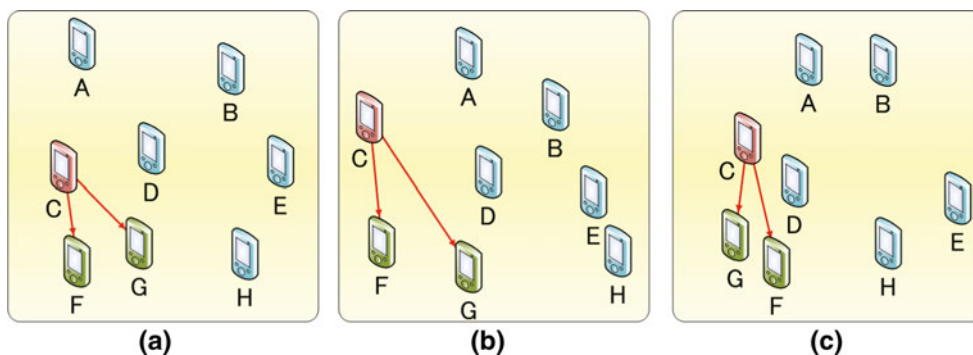
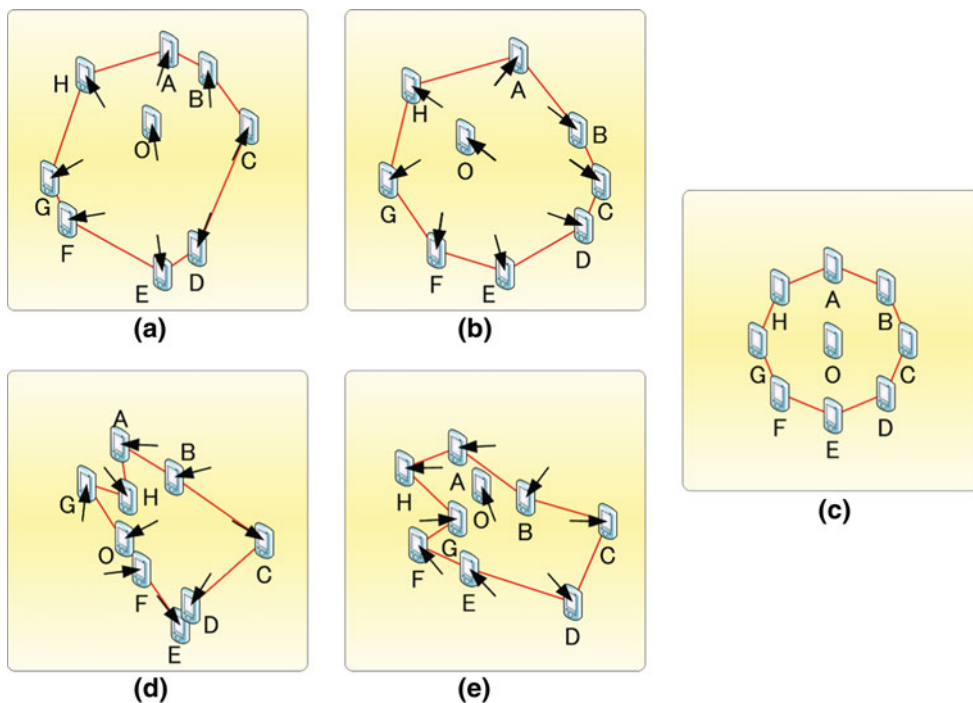


Fig. 3 Comparison of relative positions: **a, b** consistent estimations, **c** real position, **d, e** inconsistent estimation. Arrows indicate real positions of each node



true positions, node *O* seems surrounded by the other nodes, but Fig. 3(d), (e) never indicate such “relationship” among neighbors.

We try to define such position relationship dissimilarity that affects identification of nodes. The position relationship is usually defined by relations among neighboring nodes, but we need to define necessary and sufficient “neighbors” in the context of node identification.

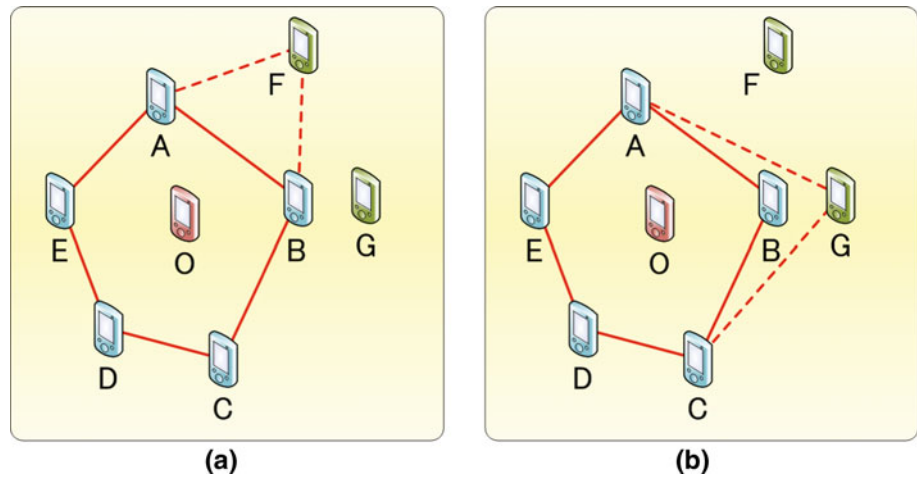
Let us consider identifying node *O* in Fig. 4(a) by regarding a set of its “neighbors” as reference points. The set $\{A, B, C, D, E, F\}$ where each node is close to *O* is a possibility, but *F* may be redundant since having *A* and *B* in the set may be sufficient to identify *O*. This concept is called *uniqueness*. The uniqueness is defined for a node in a node set and the node is called *unique* if there is no alternative in the node set. In the example, the pair of *A* and *B* may be substituted for *F*’s role of a reference point and therefore *F* is not unique in $\{A, B, C, D, E, F\}$.

$\{A, B, C, D, E\}$ is such a set of nodes where each node satisfies the uniqueness. Even though all the nodes in a node set is unique, it does not mean the uniqueness of the node set itself. For example, different node set $\{A, C, D, E, G\}$ shown in Fig. 4(b) is also such a node set. To distinguish these node sets and to choose the best one, we introduce *proximity* to *O*, i.e. the closer one to *O* should be prioritized. In this case, $\{A, B, C, D, E\}$ is better than $\{A, C, D, E, G\}$.

3.2 Definition of position relationship dissimilarity

Based on the illustrative examples, we know that a set of neighbors that satisfies the above uniqueness and proximity simultaneously should be chosen. For this purpose, we introduce the *proximity–uniqueness* concept hereafter. We define the property of proximity–uniqueness with respect to node *O* as follows.

Fig. 4 “Neighbor” sets of node O : $\{A, B, C, D, E\}$. **a** Node F is not a neighbor of node O due to node A, B , **b** Node G is not a neighbor of node O due to node B



Definition 1 Let V and $N(O)$ denote the set of all the nodes and the set of node O 's neighbors, respectively. We define a necessary and sufficient condition for node X to be an element of $N(O)$ as follows.

$$X \in N(O) \Leftrightarrow \text{for each } Z \in V - \{X, O\}, \\ \exists Y \in N(O) - \{X\}, f(\triangle OYX) \leq f(\triangle OYZ)$$

Let us assume that f represents X 's negative “proximity–uniqueness” using some neighbor $Y \in N(O)$ (larger f means less “proximity–uniqueness”). Then the definition means that X is a neighbor if and only if the pair of X and some other neighbor Y achieve better proximity–uniqueness than any other pair of Z and Y . We regard $N(O)$ that satisfies this condition as the best set of neighbors of O .

Finally, we need to define function f to represent the proximity–uniqueness. More concretely, f is a function of triangles and should return the negative degree of the proximity–uniqueness of X with respect to O and Y than any other node Z . For the objective, we define the value of $f(T)$ as the circumradius of given triangle T . In this case, as shown in Fig. 5, X is chosen as a neighbor of O based on the proximity and uniqueness as follows.

1. (Proximity) when node E of Fig. 5(a) is regarded as Z in Definition 1, there exists X such that the circumradius of triangle OYX is smaller than that of triangle OYE . Therefore, E cannot be a neighbor in the presence of X .
2. (Uniqueness) when node D of Fig. 5(b) is supposed to be Z in Definition 1, the circumradius of triangle OYX is smaller than that of triangle OYD . Moreover, X is located in the circumcircle of OYD and no node can make a smaller circumcircle with Y and O . Therefore, X cannot be replaced by any other node due to its uniqueness to Y and O .

In order to prove validity of the proposed criteria with respect to human perception, we will show the results from real experiments based on a questionnaire in Sect. 5. The set of triangles determined by function f which returns the circumradius is exactly equal to that of triangles derived by using the Delaunay triangulation algorithm [16]. We note that since a Delaunay triangulation is always unique for a given set of nodes, its corresponding $N(O)$ is also unique.

Therefore, we define the position relationship dissimilarity between a true position set and an estimated position set (usually given by a localization algorithm) as the degree of discrepancy (DoD) of Delaunay triangles formed on those sets. We define DoD by graph edit distance (GED) [17], which represents the minimum number of edge insertion and deletion required to transform one graph into the other. GED indicates the possible number of incorrect identification. Let E_r and E_e denote the sets of Delaunay edges in true positions and estimated positions, respectively. Also the Delaunay diagrams on true positions and estimated positions are denoted as $G_r = (V, E_r)$ and $G_e = (V, E_e)$, respectively. The GED between G_r and G_e is defined as follows.

$$\text{Graph edit distance} = \frac{\sum_{X,Y \in V} \text{GED}(X, Y)}{2}$$

$$\text{GED}(X, Y) = \begin{cases} 1 & \text{if } (X, Y) \in E_r \wedge (X, Y) \notin E_e \\ & \vee (X, Y) \notin E_r \wedge (X, Y) \in E_e \\ 0 & \text{otherwise} \end{cases}$$

We use a normalized value of GED to define DoD. When E_e does not include any edges in E_r , GED takes the maximum value of $|E_r| + |E_e|$. Hence we define DoD as

$$\text{DoD} = \frac{\text{Graph edit distance}}{|E_r| + |E_e|}$$

In the example of Fig. 6, common edges between G_r (left) and G_e (right) are shown by solid lines. There are

Fig. 5 Neighbors definition based on circumscribed circles: **a** node E is not a neighbor of node O because the radius of $\triangle OYE$ is longer than that of $\triangle OYX$. **b** Node X is a neighbor of node O because the radius of $\triangle OYX$ is shorter than that of $\triangle OYD$

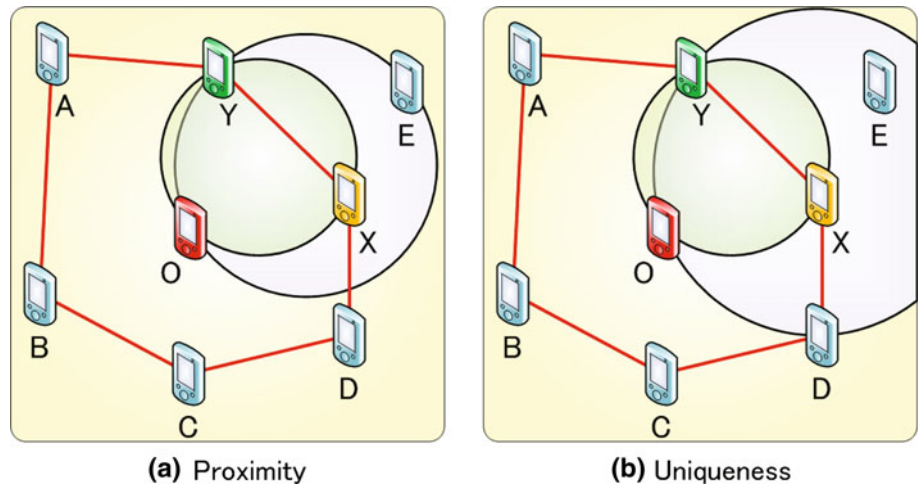
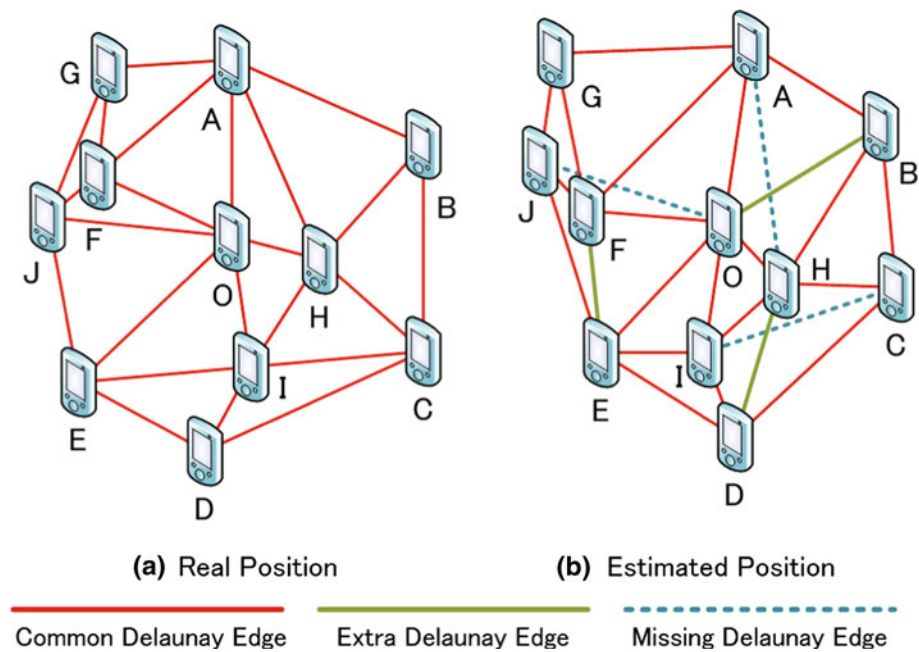


Fig. 6 An example of discrepancy between Delaunay triangulations: links OB , DH , and BF are extra Delaunay edges and links OJ , AH , and CI are missing Delaunay edges



three missing edges (shown by dotted lines) and three extra edges (shown by dashed lines) in G_e . Thus GED is 6 in this case and DoD becomes $\frac{6}{23} \simeq 0.26$. We note that when DoD is equal to 0, all Delaunay edges in E_e correspond to the Delaunay edges in E_r . Thus all neighbors of each node in the estimated positions completely match those in the real positions. As DoD approaches to 1, it is harder to identify nodes from the estimated positions.

We assume there is no need to calculate DoD in real time since DoD is expected to be used for choosing the best localization algorithms before running location-based systems. Nevertheless, we discuss the computational complexity of the proposed method. The computation of Delaunay Triangulations requires $O(n \log n)$ while that of graph edit distance is $O(n^2)$ where n is the number of

nodes. Therefore, the computational complexity is $O(n^2)$. This indicates it is also possible to compute DoD in real time if needed.

4 Additional important criteria

In this section, we discuss other criteria that should also be considered to capture human perception as well as the Delaunay triangulation.

4.1 Viewpoint location

We have defined DoD based on bird's-eye view (i.e. 2D-DoD). However, its 3D version (3D-DoD) should also

Fig. 7 Effect of different viewpoints

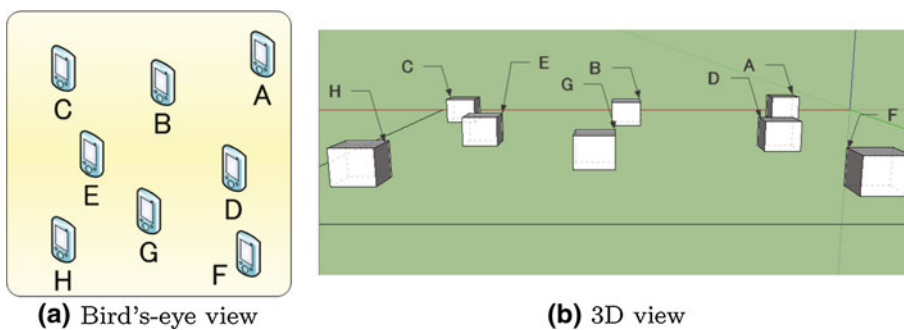
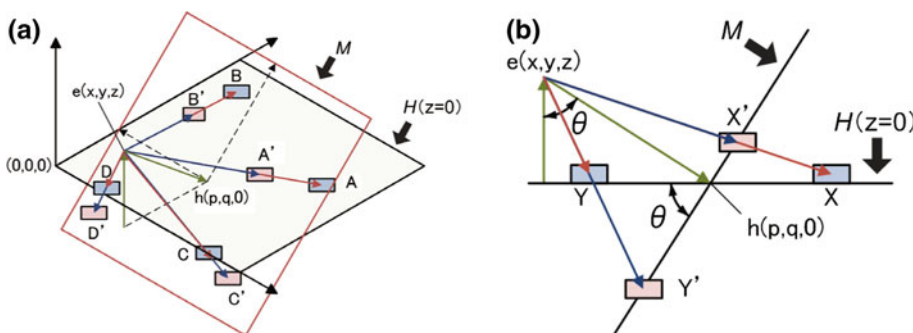


Fig. 8 Transformation with viewpoint: **a** objects $A, B, C,$ and D on plane H are projected to objects $A', B', C',$ and D' on plane M which is perpendicular to the line of sight. **b** Projection of A and C seeing from the side



be designed to consider viewpoint location in the real world. In applications such as a storehouse example shown in Fig. 1, estimation results are shown to users in a target field. In such cases, object deployment seems different depending on viewpoints of users. The major effect of viewpoints is that distance between nearby objects appears to be longer than that between distant objects. For example, distance between node F and H is shorter than that between A and C in the bird's-eye view shown in Fig. 7(a). However, distance between node F and H becomes longer than that between A and C in 3D view (see Fig. 7(b)).

In order to define DoD considering such viewpoint effects, we transform the ground plane (2D-plane) to another plane in a 3D space by using the line of sight. Suppose that the target region is a ground region H where a viewpoint is at $e = (x, y, z)$ and the eyes are looking at a point $h = (p, q, 0)$ in region H as shown in Fig. 8(a). We introduce the oblique region M which is perpendicular to \vec{eh} (the line of sight) and contains h . Then node positions $A, B, C,$ and D on H are projected onto M . We consider rays from the viewpoint e to each node position. Finally, we map node positions $A, B, C,$ and D on H to intersections $A', B', C',$ and D' of M and the rays, respectively. For example, Fig. 8(b) shows projection of A and C seeing from the side. The distance between A and h is equal to that between C and h on H . However, after projection onto M , distance between A' and h becomes shorter than that between C' and h as shown in the figure. By the above transformation, we can apply our approach to location-based applications affected by viewpoints in a 3D space.

We note that the correspondence between the bearings of real/estimated positions is assumed to be known.¹ This is usually done by referring to absolute reference points on the ground (e.g. buildings and signs in real world's views) or digital compasses in mobile devices.

4.2 Nodes in close proximity

In human perception, nodes in close proximity are regarded as a cluster (i.e. group) [15]. Since those nodes in the same cluster are too close to each other, they may not be necessary to be distinguished in most realistic applications and situations. Meanwhile, if *organization* of clusters in estimated positions is quite different from that in true positions, it significantly affects identification accuracy.

Therefore, we quantify the degree of discrepancy between two cluster organizations in real and estimated positions. For this purpose, we propose a clustering algorithm that fits for human perception and introduce a similar idea to the graph edit distance in the Delaunay triangulations. We note that the existing clustering algorithms [18–21] are classified into hierarchical or non-hierarchical algorithms. In non-hierarchical algorithms such as [19], the number of clusters must be specified before clustering nodes. However, since clustering based on human perception largely depends on the distribution of nodes, it is

¹ Without this assumption, identification becomes very hard since rotation should be considered.

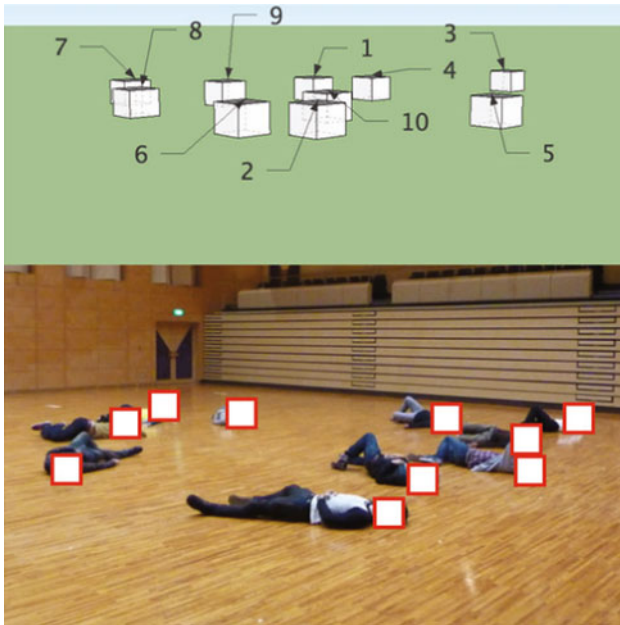


Fig. 9 Example of questionnaire: picture shows estimated positions of 10 objects. Photograph showing real positions of corresponding 10 persons. Subjects are required to guess IDs of each person

hard to specify the number of clusters beforehand, and hierarchical algorithms such as [20] are more appropriate.

Based on informal interviews with emergency medical doctors who are our collaborators in the emergency rescue support project [22] and actually need identification of injured people in disaster sites, we recognize that *inter-cluster distance* is a significant factor. We take from the existing clustering algorithm a strategy that renders this factor.

To consider inter-cluster distance, we introduce the group average method [21] which uses the average distance between nodes in two different clusters as the inter-cluster distance. Inter-cluster distance $d(C_1, C_2)$ of clusters C_1 and C_2 is defined as:

$$d(C_1, C_2) = \frac{1}{|C_1||C_2|} \sum_{p \in C_1} \sum_{q \in C_2} d(p, q) \quad (1)$$

where $|C_1|$ and $|C_2|$ respectively denote the number of nodes in C_1 and C_2 , and $d(p, q)$ is the Euclidean distance between nodes p and q .

[Clustering Algorithm]

(Step 1) Let N be the number of nodes. Initialize the set \mathcal{C} of clusters to N clusters where each cluster has one node.

(Step 2) For clusters C_1 and C_2 in \mathcal{C} with the shortest inter-cluster distance, check if $d(C_1, C_2)$ is less than threshold α or not. If true, merge C_1 and C_2 in \mathcal{C} and go to Step 2. Otherwise terminate the algorithm. Empirically α should be less than 1 m and $\alpha = 0.6$ m was used in the following experiments.

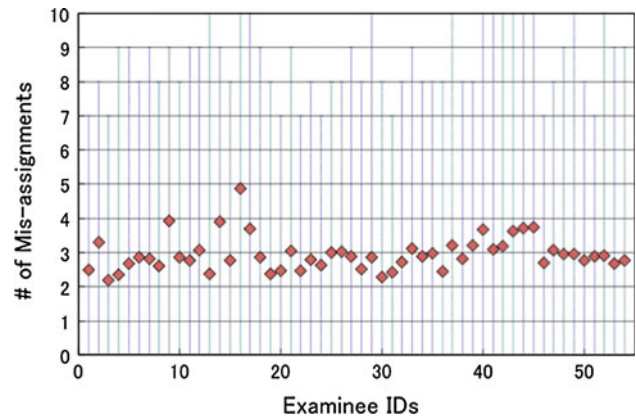


Fig. 10 # of mis-assignments of 54 subjects. Each *dot* indicates averages of mis-assignments and each *line* shows ranges of mis-assignments

We tailor DoD defined in Sect. 3.2 such that it can incorporate the clustered nodes. Firstly, we organize the clusters over real positions using the above algorithm. Then we apply the same cluster organization to estimated positions. Regarding the centroid of each cluster as the location of the cluster, we build the Delaunay triangles on real and estimated clusters and compare them to derive DoD.

5 DoD and identification accuracy correlation

We have conducted an experiment to see the correlation between DoD and human intuition. In the experiment, we have prepared 30 pairs of real positions and their corresponding estimated positions of 10 nodes (actually they are 10 students). Eyepoints in estimation results were set to the 4 corners of the area with 170 cm height. Therefore, we have prepared 120 pairs as a total and 54 examinees participated in this experiment. As a total, we had 6,480 answers for 120 questionnaires.

An example questionnaire is shown in Fig. 9 where node IDs were shown in the estimated positions but hidden in the real positions. For real positions, we have used the pictures of 10 students lying on the floor. Such a situation is likely to happen in emergency sites where injured persons are waiting to be treated and delivered to hospitals [22]. Given a pair of position sets, each examinee was required to identify node IDs in the real positions. The correctness of the answer is observed by the number of mis-assignments in each pair.

In order to examine the individual variability before the analysis of results, we summarized the average number of mis-assignments with error bars for each examinee. From the result shown in Fig. 10, we can see that the average number of mis-assignments is very similar among

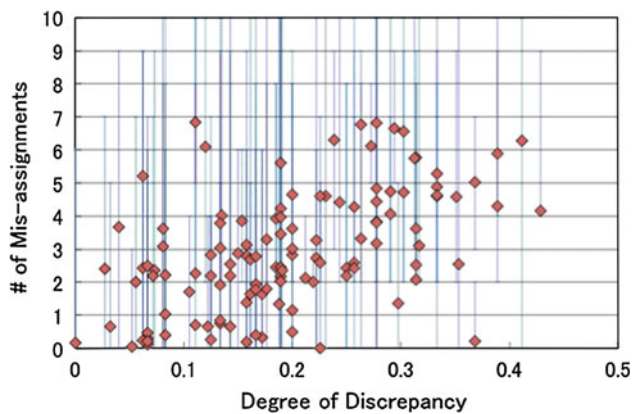


Fig. 11 DoD versus # of mis-assignments. Each dot indicates averages of mis-assignments and each line shows ranges of mis-assignments

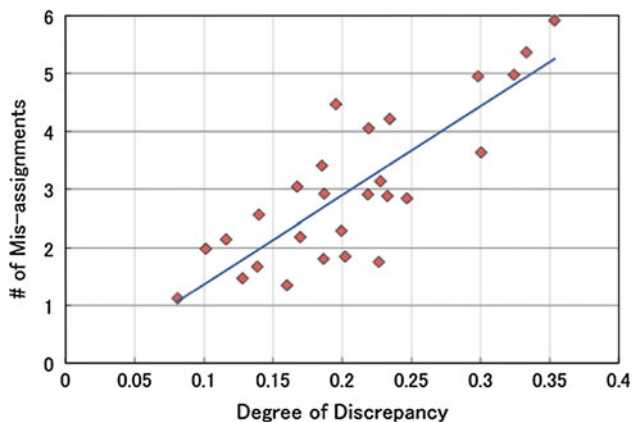


Fig. 12 Avg. DoD versus # of mis-assignments. The line indicates straight-line approximation

examinees and it is not necessary to take individual variability into account. We note that for the same questionnaire, there is of course variability among examinees. Even though it is mostly impossible to disregard such variability for different types of questionnaires, the data in Fig. 10 is helpful to analyze DoD trend in the followings and to justify the uniformity of the dataset among the examinees.

Figure 11 shows the number of mis-assignments with error bars for each DoD value. Due to difference among questionnaires and viewpoints, the range of mis-assignments for the same DoD value seems spread. However, we can see certain trend of mis-assignment growth along with DoD where the trend more clearly appears on the average values.

In order to make this trend more visible, we have taken the averages of DoDs and the number of mis-assignments over the 13 different examinees and 4 different eyepoints. From the resulting 30 cases, we have discarded 10 % to avoid outliers and finally 27 cases were left in Fig. 12.

We have also calculated the correlation coefficient and it was 0.82, which generally indicates strong relationship.

6 Analysis of localization algorithm by DoD

In the last section, we have shown that DoD could capture human perception in identifying object location. Based on this, we characterize different types of localization algorithms and analyze their localization “accuracy” in terms of object identification.

6.1 Localization algorithms to be examined

We have selected (a) GPS as a non-cooperative, range-based positioning system, (b) MDS-MAP [23] as a multi-hop, range-based cooperative localization algorithm, and (c) TRADE [10] as a multihop, range-free cooperative localization algorithm that utilizes connectivity information. This is reasonable selection where we can see the characteristics of different localization algorithms on DoD through comparison between (1) non-cooperative and cooperative algorithms, and (2) range-based and range-free algorithms. Although we have not selected an algorithm from the non-cooperative range-free category, we can suppose its characteristic from the above comparison.

In non-cooperative range-based techniques such as GPS, each node independently estimates its own position by using direct measurement from reference points. MDS-MAP is a localization algorithm based on multi-dimensional scaling [24]. MDS-MAP exploits estimated distances between nodes based on received signal strength (RSS). Then the positions of nodes are estimated by matrix calculations with constraints on distances among nodes. Euclid distance between nodes is approximated by network hop counts and estimated per-hop distance.

Finally, TRADE is a localization algorithm using internode connectivity information. Nodes in TRADE continue adjusting their positions and past trajectories to fit for spatial constraints from the maximum communication range and maximum movement speed.

6.2 Simulation settings

The default values of simulation parameters are shown in Table 1. Four viewpoints were set at the corners of the target region with 170 cm height. To generate GPS errors, we have given both distance and directional errors for each true position which were randomly selected in $[0, e_g]$ and $[0, \theta]$, respectively. Then GPS has been examined with the maximum distance error $e_g \in [0.4, 2.8\text{m}]$ with step 0.8 m and the angle error $\theta = [0.5\pi, 2.0\pi]$ with step 0.5π . MDS-MAP has been examined with three distributions of

Table 1 Simulation parameters

Area size	10 (m) × 10 (m)
# of landmarks	4
# of nodes	30
Node mobility	Random waypoint
Moving speed	1.0–1.5 (m/s)
Pause time	0 (s)
Simulation time	100 (s)
Clustering threshold (α)	0.6 (m)

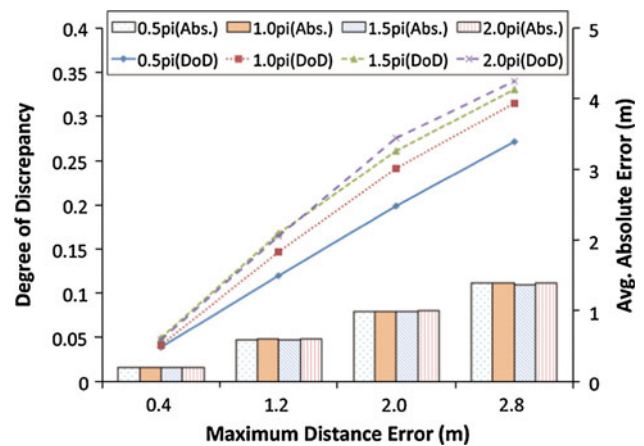
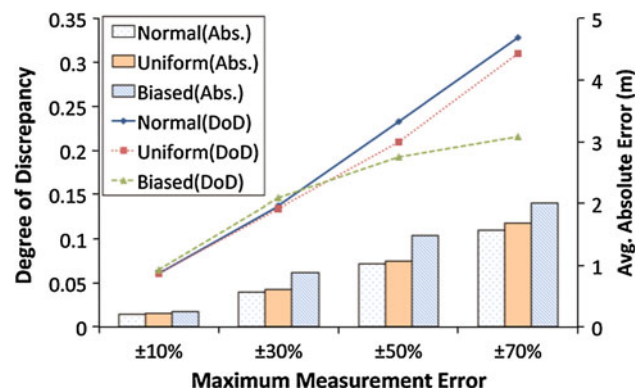
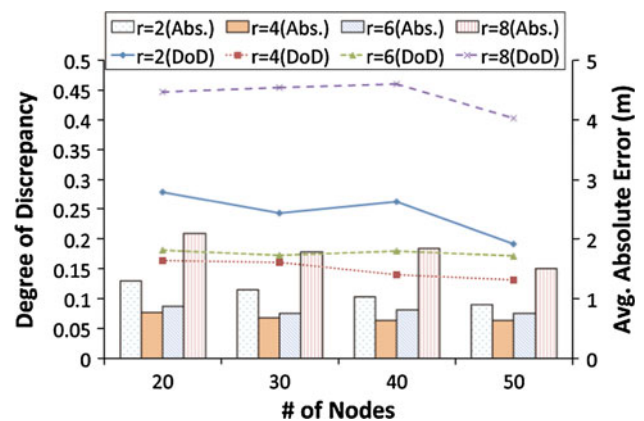
measurement errors; uniform, normal and biased distributions with the “maximum measurement error” e_m , which is given as a ratio to true distances. In the uniform distribution, the measurement error was determined by randomly choosing values from $[-e_m, e_m]$. In the normal distribution, the measurement error followed the normal distribution with mean 0 and $\sigma = e_m/2$. In the biased distribution, it was determined by randomly choosing values from $[-e_m, -e_m + 0.05]$ and $[e_m - 0.05, e_m]$ (errors stick around $\pm e_m$ with 5 % deviation). In TRADE, the number of nodes was selected from 20, 30, 40, and 50, and communication range r was set to 2, 4, 6, or 8 m.

In comparison between different localization algorithms in Sect. 6.4, the area size was set to 25 m × 25 m and the number of nodes was 20. In GPS, distance and directional errors were randomly selected from the range [0 m, 3 m] and $[0, 2.0\pi]$, respectively. We randomly selected distance measurement errors in MDS-MAP from the range $[-10, 10\%]$ and used 10m of communication range r in TRADE.

6.3 DoD characteristics of different localization algorithms

Fig. 13 shows DoDs versus the maximum distance error e_g in GPS. The bar chart indicates the average distance errors using the right Y-axis (i.e. it shows not “relative errors” but “absolute errors”). The important point is that although the absolute errors are almost equal among different angle errors in $[0.5\pi, 2.0\pi]$, DoDs shown by the line chart using the left Y-axis show different values and trends. Since angle errors significantly affect the relative location of nodes, a larger angle error should generally indicate more rapid growth of DoD. This property can be observed in the DoD line chart, and we can say that DoD can distinguish such errors that are caused by directional errors.

Figure 14 shows DoDs versus the maximum distance error e_m in MDS-MAP. Similarly with the GPS case, the absolute errors are shown by the bar chart using the right Y-axis. The interesting characteristics are found in the biased distribution where the absolute errors are largest but DoDs are smallest with larger e_m (50 and 70 %). Since biased

**Fig. 13** Maximum distance error e_g in GPS versus DoD and absolute error**Fig. 14** Maximum measurement error e_m in MDS-MAP versus DoD and absolute error**Fig. 15** # of nodes in TRADE versus DoD and absolute error

distribution generated almost two constant values as errors ($\pm e_m$ with small deviations), in the most part the position relationships were kept intact under large absolute errors. As in the GPS case, we could observe that DoD could capture such a property.

Fig. 16 Estimated positions by different localization algorithms. Each *line* indicates the distance and angle error of each node in estimated positions

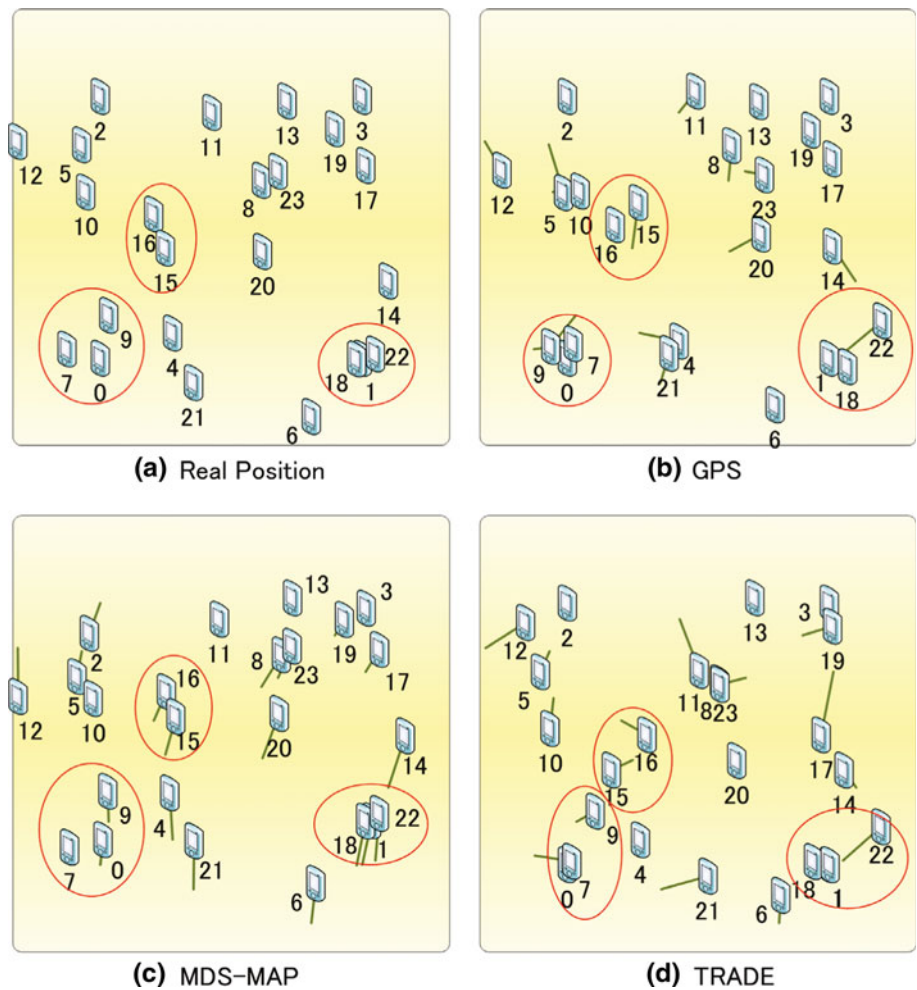


Table 2 Position errors of localization algorithms

	GPS	MDS-MAP	TRADE
Absolute error (per R)	0.168	0.188	0.154
Degree of discrepancy	0.331	0.127	0.246

Finally, DoDs versus the number of nodes in the case of TRADE are shown in Fig. 15. Overall, the absolute errors of TRADE decrease with the increase of node density because the amount of spatial constraints increases. Communication ranges also affect absolute errors since a larger communication range may increase connectivity. However, the large communication range may also increase absolute errors since it may relax spatial constraints. When the communication range was 2 m, the absolute error was the second worst among the four ranges because the range was too small to constrain the location of other nodes. Here, due to the feature of range-free algorithms where relative positions are not preserved strictly, the position relationship is also affected by the evaluated factors, i.e. node density and communication range. In this context, DoDs follow the similar trend of the absolute errors, which is natural.

6.4 Comparison between different localization algorithms

Figure 16(b), (d) show snapshots of estimated positions of the three algorithms and their real positions are shown in Fig. 16(a) when the number of nodes is 20 with 4 landmarks (IDs 0–3). The absolute errors are shown by segments from each node. We can see the difference in relative positions between these algorithms, especially for nodes marked by circles in the snapshots. Relative positions in MDS-MAP (Fig. 16(c)) are very close to those in the real positions (Fig. 16(a)).

Table 2 also describes the absolute and relative errors at that time. Surprisingly, MDS-MAP is the best in the relative error but the worst in the absolute error. This means relative errors cannot be measured by absolute errors only. Therefore, it is important to evaluate localization algorithms in terms of relative errors depending on services and applications. From the above results, we have confirmed that DoDs could represent the different characteristics of localization algorithms in terms of position relationship.

7 Conclusion

In this paper, we have proposed a method to quantify localization accuracy in terms of object identification. We have analyzed primary factors that affect object identification and have found that the Delaunay triangulation could capture such factors. We have also analyzed additional factors such as eyepoints and grouping. By subjective testing based on 120 questionnaires by 54 examinees with 6,480 answers, we have justified our proposed metric, i.e. degree of discrepancy (DoD) between the real and estimation positions. Simulation results have also shown that DoD could capture the different characteristics of localization algorithms which have not been found by absolute errors. We believe that new emerging mobile and pervasive applications such as AR-based navigation are beneficial from our approach to assess adequacy of positioning systems they use.

Acknowledgments This research was supported by JST, CREST.

References

1. Olguin, D. O., Waber, B. N., Kim, T., Mohan, A., Ara, K., & Pentland, A. (2009). Sensible organizations: Technology and methodology for automatically measuring organizational behavior. *IEEE Transactions on Systems, Man, and Cybernetics, Part B: Cybernetics*, 39(1), 43–55.
2. Lukowicz, P., Timm-Giel, A., Lawo, M., & Herzog, O. (2007). WearIT@work: Toward real-world industrial wearable computing. *IEEE Pervasive Computing*, 6(4), 8–13.
3. Yang, Z., & Liu, Y. (2010). Quality of trilateration: Confidence-based iterative localization. *IEEE Transactions on Parallel and Distributed Systems*, 21(5), 631–640.
4. Ash, J. N., & Moses, R. L. (2008). On the relative and absolute positioning errors in self-localization systems. *IEEE Transactions on Signal Processing*, 56(11), 5668–5679.
5. Matsakis, P., & Wendling, L. (1999). A new way to represent the relative position between areal objects. *IEEE Transactions on Pattern Analysis and Machine Intelligence*, 21(7), 634–643.
6. Priyantha, N. B., Chakraborty, A., & Balakrishnan, H. (2000). The cricket location-support system. In *Proceedings of the MobiCom* (pp. 32–43).
7. Place engine. <http://www.placeengine.com/en>.
8. Shang, Y., Ruml, W., Zhang, Y., & Fromherz, M. P. J. (2003). Localization from mere connectivity. In *Proceedings of the ACM MobiHoc* (pp. 201–212).
9. Nagpal, R., Shrobe, H., & Bachrach, J. (2003). Organizing a global coordinate system from local information on an ad hoc sensor network. In *Proceedings of the information processing in sensor networks* (pp. 333–348).
10. Fujii, S., Nomura, T., Umedu, T., Yamaguchi, H., & Higashino, T. (2009). Real-time trajectory estimation in mobile ad hoc networks. In *Proceedings of the ACM international conference on modeling, analysis and simulation of wireless and mobile systems* (pp. 163–172).
11. Turk, M., & Pentland, A. (1991). Face recognition using eigenfaces. In *Proceedings of the IEEE conference on computer vision and pattern recognition* (pp. 586–591).
12. Demirci, M. F., Platel, B., Shokoufandeh, A., Florack, L. L. M. J., & Dickinson, S. J. (2009). The representation and matching of images using top points. *Journal of Mathematical Imaging and Vision*, 35(2), 103–116.
13. Bebis, G., Deaconu, T., & Georgiopoulos, M. (1999). Fingerprint identification using Delaunay triangulation. In *Proceedings of the IEEE international conference on intelligence, information and systems* (pp. 452–459).
14. Papari, G., & Petkov, N. (2005). Algorithm that mimics human perceptual grouping of dot patterns. In *Proceedings of the international symposium on brain, vision and artificial intelligence* (Vol. 3704, pp. 497–506).
15. Wertheimer, M. (1938). Laws of organization in perceptual forms. *A Sourcebook of Gestalt Psychology*, 71–88.
16. Lee, D.T., & Schachter, B.J. (1980). Two algorithms for constructing a Delaunay triangulation. *International Journal of Parallel Programming*, 9(3), 219–242.
17. Bunke, H. (1997). On a relation between graph edit distance and maximum common subgraph. *Pattern Recognition Letters*, 18(8), 689–694.
18. Murtagh, F. (1983). A survey of recent advances in hierarchical clustering algorithms. *The Computer Journal*, 26(4), 354–359.
19. Macqueen, J. B. (1967). Some methods of classification and analysis of multivariate observations. In *Proceedings of the Berkeley symposium on mathematical statistics and probability* (pp. 281–297).
20. Ward, J.H. (1963). Hierarchical grouping to optimize an objective function. *Journal of the American Statistical Association*, 58(301), 236–244.
21. Sokal, R.R., & Michener, C.D. (1958). A statistical method for evaluating systematic relationships. *University of Kansas Scientific Bulletin*, 28, 1409–1438.
22. E-triage project. <http://www.higashi.ist.osaka-u.ac.jp/research/e-triage.html>.
23. Shang, Y., Ruml, W., Zhang, Y., & Fromherz, M. (2004). Localization from connectivity in sensor networks. *IEEE Transactions on Parallel and Distributed Systems*, 15(11), 961–974.
24. Carroll, J. D., & Chang, J. J. (1970). Analysis of individual differences in multidimensional scaling via an N-way generalization of Eckart-Young decomposition. *Psychometrika*, 35(3), 283–319.

Author Biographies



Noboru Kiyama received the ME degree in Information and Computer Science from Osaka University, Japan in 2010. He is currently a researcher at Hitachi, Ltd. and also a doctoral student at Osaka University. His current research interests include Telematics services for electric vehicles. He is a member of Information Processing Society of Japan (IPSJ).



Akira Uchiyama received the ME and Ph.D. degrees in Information and Computer Science from Osaka University, Japan in 2005 and 2008, respectively, and is currently an Assistant Professor at Osaka University. He was a visiting scholar in University of Illinois at Urbana- Champaign in 2008 and a research fellow of the Japan Society for the Promotion of Science from 2007 to 2009. His current research interests include modeling, design and development of wireless

network applications. He is a member of IEEE and Information Processing Society of Japan (IPSJ).



Hirozumi Yamaguchi received his BE, ME and Ph.D. degrees in Information and Computer Sciences from Osaka University, Japan in 1994, 1996 and 1998, respectively. He is currently an Associate Professor at Osaka University. His current research interests include design, development, modeling and simulation of mobile and wireless networks and applications. He is a member of IEEE.



Teruo Higashino received his BS, MS and Ph.D. degrees in Information and Computer Sciences from Osaka University, Japan in 1979, 1981 and 1984, respectively. He joined the faculty of Osaka University in 1984. Since 2002, he has been a Professor in Graduate School of Information Science and Technology at Osaka University. His current research interests include design and analysis of distributed systems, communication protocol and mobile computing.

He is a senior member of IEEE, a fellow of Information Processing Society of Japan (IPSJ), and a member of ACM and IEICE of Japan.